A R C H I V E S O F M E T A L L U R G Y A N D M A T E R I A L S
Volume 59 2014 Issue 3
DOI: 10.2478/amm-2014-0143

Z. HUDA*, T. ZAHARINIE**, I.H.S.C. METSELAAR**, S. IBRAHIM**, GOH J. MIN**

KINETICS OF GRAIN GROWTH IN 718 Ni-BASE SUPERALLOY

KINETYKA WZROSTU ZIAREN W NADSTOPIE NIKLU 718

The Haynes® 718 Ni-base superalloy has been investigated by use of modern material characterization, metallographic and heat treatment equipment. Grain growth annealing experiments at temperatures in the range of 1050-1200°C (1323-1473K) for time durations in the range of 20 min-22h have been conducted. The kinetic equations and an Arrhenius-type equation have been applied to compute the grain-growth exponent n and the activation energy for grain growth, Q_g, for the investigated alloy. The grain growth exponent, n, was computed to be in the range of 0.066-0.206; and the n values have been critically discussed in relation to the literature. The activation energy for grain growth, Q_g, for the investigated alloy has been computed to be around 440 kJ/mol; and the Q_g data for the investigated alloy has been compared with other metals and alloys and ceramics; and critically analyzed in relation to our results.

Keywords: Nickel-base superalloy; microstructures; grain growth; kinetics; activation energy

Nadstop na bazie niklu Haynes® 718 badano przy użyciu nowoczesnych urządzeń do charakterystyki materiałów, metalografii i obróbki cieplnej. Przeprowadzono badania wzrostu ziarna podczas wyżarzania w zakresie temperatur 1050-1200°C (1323-1473K) w czasie trwania od 20 minut do 22 godzin. Równania kinetyczne i równanie typu Arrheniusa zostały zastosowane do obliczania wykładnika wzrostu ziarna n oraz energii aktywacji wzrostu ziarna Q_g, dla badanego stopu. Obliczona wartość wykładnika wzrostu ziarna n, mieści się w zakresie od 0,066 do 0,206 i została krytycznie przedyskutowana w odniesieniu do literatury. Obliczona energia aktywacji wzrostu ziaren Q_g, wynosi dla badanego stopu na około 440 kJ/mol. Dane Q_g dla badanego stopu porównywano z danymi dla innych metali, stopów i ceramiki oraz krytycznie analizowano w odniesieniu do naszych wyników.

1. Introduction

Although substantial research has been conducted on the γ' particle-coarsening behavior (*e.g.* [1], [2], [3], [4], [5], [6], [7], [8] and [9]), limited research has been reported on the kinetics of grain growth in superalloys [10], [11], [12] and [13]. This research paper, therefore, aims to establish the kinetics of grain growth by computing the grain-growth exponent n and the activation energy of grain growth, Q_g, in the temperature range of 1373-1473K for the investigated 718 Ni-base superalloy.

Superalloys are extensively used in hot sections of gas-turbine engines owing to their excellent creep and corrosion resistance at high temperatures [11], [14], [15], [16] and [17]. In particular, the 718 nickel-base superalloy has a lower cost as compared to other superalloys resulting in a wider spread use of this superalloy [18]. The control and kinetics of grain growth in superalloys are of great technological importance because superalloys are high-temperature materials, and since many material properties are strongly dependant on grain size [10] and [15]. Grain growth is the post-recrystallization stage of annealing. In general, recrystallization starts at a temperature around $0.4T_m$ (T_m = melting temperature measured in K); and the melting temperature for IN 718 superalloy is in the range of 1533-1609K [19]. Grain growth occurs in polycrystalline materials to maintain their thermodynamic stability by reducing their grain boundary energy, thereby reducing the total energy of the system. The grain boundary area is in a high-energy state and this energy is proportional to the driving force for the grain growth. Therefore the driving force for grain growth varies as the inverse of the grain size [20].

The kinetics of normal grain growth assumes a linear relationship between growth rate and the inverse of grain size; which is proportional to the grain diameter as follows [21]:

$$\frac{dD}{dt} = \frac{k}{D} \tag{1}$$

where D is the mean grain diameter after an annealing time t at temperature T, and k is a temperature-dependent rate constant.

On integration, Equation (1) takes the form **[21]**:

$$D_t - D_0 = kt^n \tag{2}$$

* DEPARTMENT OF ENGINEERING, NILAI UNIVERSITY, NILAI, 71800 NEGERI SEMBILAN, MALAYSIA
** DEPARTMENT OF MECHANICAL ENGINEERING, UNIVERSITY OF MALAYA, 50603 KUALA LUMPUR, MALAYSIA

TABLE 1

Chemical composition of the Haynes 718 Ni-base superalloy

Elements	Ni	G	Al	Ti	Mo	B	C	Si	Co	Cu	Mn	Fe	P	S
wt%	53.10	18.40	0.56	1.00	3.07	0.003	0.054	0.09	0.16	0.10	0.26	balance	<0.005	0.002

where D_0 is the pre-growth grain diameter, D_t is the grain diameter at any instant t during grain growth, n is the grain growth exponent and k is a constant depending on the metal's composition and annealing temperature.

In logarithmic form, Equ. (2) can be expressed as follows:

$$\log(D_t - D_0) = \log k + n \log t \tag{3}$$

Equation (3) enables us to graphically compute the grain-growth exponent, n.

The rate of grain growth, G, can be expressed by the relation:

$$G = (D_2 - D_1)/(t_2 - t_1) \tag{4}$$

where D_1 is the mean grain diameter after annealing for the time duration t_1 and D_2 is the mean grain diameter after annealing for the time duration t_2 at a particular temperature. Once the set of values of G have been calculated for a particular temperature, the activation energy for grain growth can be computed as follows ([22], [23] and [24]):

$$G = G_0 \exp(-Q_g/RT) \tag{5}$$

where Q_g is the activation energy for grain growth, G_0 is a new constant, and R and T have their usual meanings.

2. Experimental Work

2.1. Material

The staring material (*SM*) (HAYNES® 718 Ni-Base Superalloy) was acquired from Haynes International Inc. Alloys, USA. The *SM* was in the form of plate; the chemical composition of the *SM* is given in Table 1.

2.2. Metallographic and annealing practices

Seventeen (17) samples from the *SM* were sectioned by use of a diamond-wheel cut-off machine (facilitated with cooling fluid during the cutting operation) so as to conduct metallographic investigations on the rolling plane. Sixteen (16) samples were given grain-growth annealing heat treatments at temperatures in the range of 950°C-1300°C (1223K-1573K) for durations in the range of 20 min-22 h; and the sample identification scheme is shown in Table 2. Metallographic specimens for the as-received material as well as for the heat-treated samples were prepared.

Annealing heat-treatment experiments were conducted by use of a ***Carbolite*** tube furnace filled with nitrogen gas facilitated with a digital temperature control. The metallographic specimens for the sixteen (16) samples were prepared by metallographic grinding followed by polishing using high-alumina powder. Metallographic etching for the Ni-based alloy was accomplished using an etching solution of 20% HCl and 80% methanol. The microstructural characterization involved the use of both optical as well as scanning electron microscope (SEM) (Zeiss and Auriga SEM). The photomicrographs for the metallographic specimens were taken by use of SEM as well as by using an optical microscope linked with a computerized imaging system facilitated by the ***i-Solution*** software. The average grain diameters were measured by quantitative metallographic technique. The grain-growth exponent n at various temperatures and the activation energy for grain growth, Q_g were computed by graphical techniques.

TABLE 2

Sample identification scheme according to heat-tretment parameters

Sample ID#	Annealing parameters
A-1	1323 K / 20 min
A-2	1323 K / 20 h
A-3	1323 K / 8 h
A-4	1323 K / 22 h
B-1	1373 K / 20 min
B-2	1373 K / 20 h
B-3	1373 K / 8 h
B-4	1373 K / 22 h
C-1	1423 K / 20 min
C-2	1423 K / 20 h
C-3	1423 K / 8 h
C-4	1423 K / 22 h
D-1	1473 K / 20 min
D-2	1473 K / 20 h
D-3	1473 K / 8 h
D-4	1473 K / 22 h

3. Results and discussion

3.1. Microscopy

The scanning electron micrographs of the Haynes 718 Ni-base superalloy, in the as-received condition, are shown in Fig. 1(a-c). It can be clearly observed from the SEM micrographs that there are two distinct phases: austenite (γ) matrix and second-phase particles in the microstructure of the as-received 718 nickel-base superalloy. The average grain size was computed from the SEM micrographs [see Fig. 1(a-c)]; and the value of the grain size for the investigated superalloy, in the as-received condition, was measured to be around 15.5 14 μm.

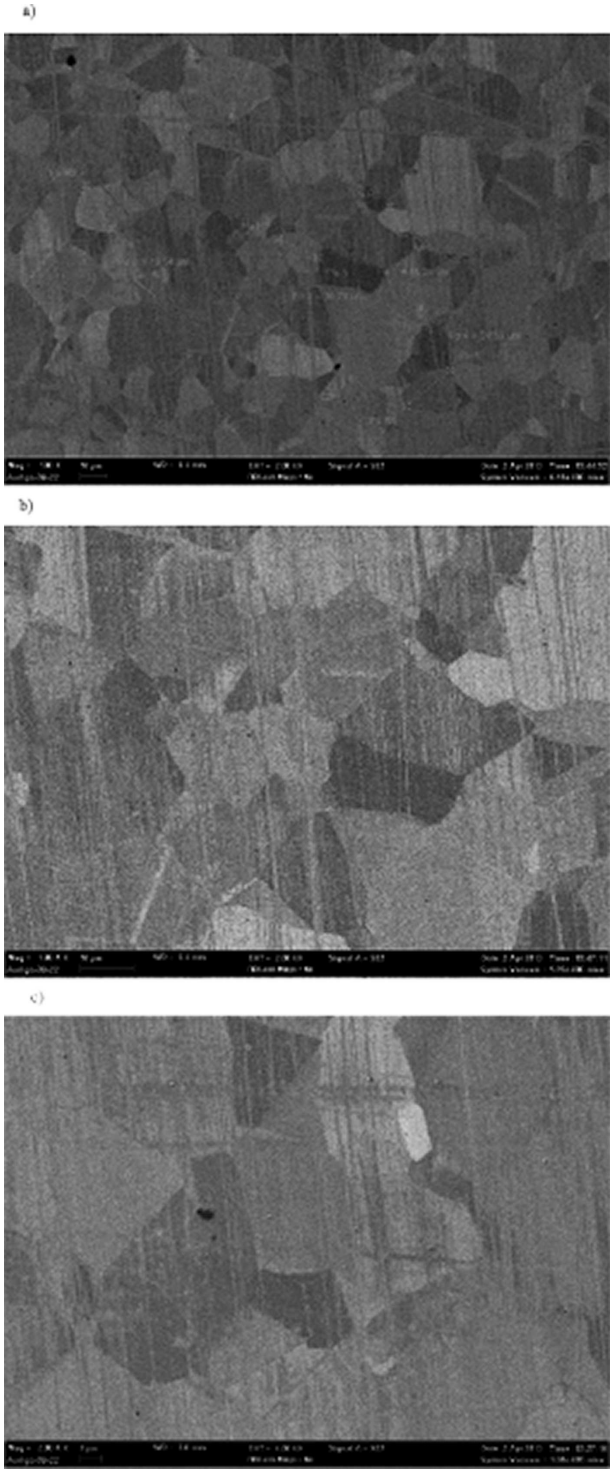

Fig. 1. (a) SEM micrograph of the as-received superalloy at Mag.: 500 X; (b) SEM micrograph of the as-received superalloy at Mag.: 1,000 X; (c) SEM micrograph of the as-received superalloy at Mag.: 2,000 X

The optical micrographs of the as-received and the annealed samples are shown in Figs 2(a-c). A comparison of the phases in microstructure of the as-received alloy, as observed in the optical micrograph (Fig. 2a) with the microstructure of the same material as observed by the SEM (Fig. 1a) confirms that there are two distinct phases: austenite (γ) matrix and second-phase particles in the microstructure of the as-received 718 nickel-base superalloy. Now, wec compare the microstructure of the as-received sample with that for the annealed samples. The optical micrographs for the annealed sample [(Figs 2(b,c)] shows an absence of the second-phase; which indicates dissolution of the second-phase particles due to the high temperature annealing at 1323K and at 1473K. Additionally, some annealing twins are also observed due the highest-temperature annealing treatment (1473K/2h) [see Fig. 2(c)].

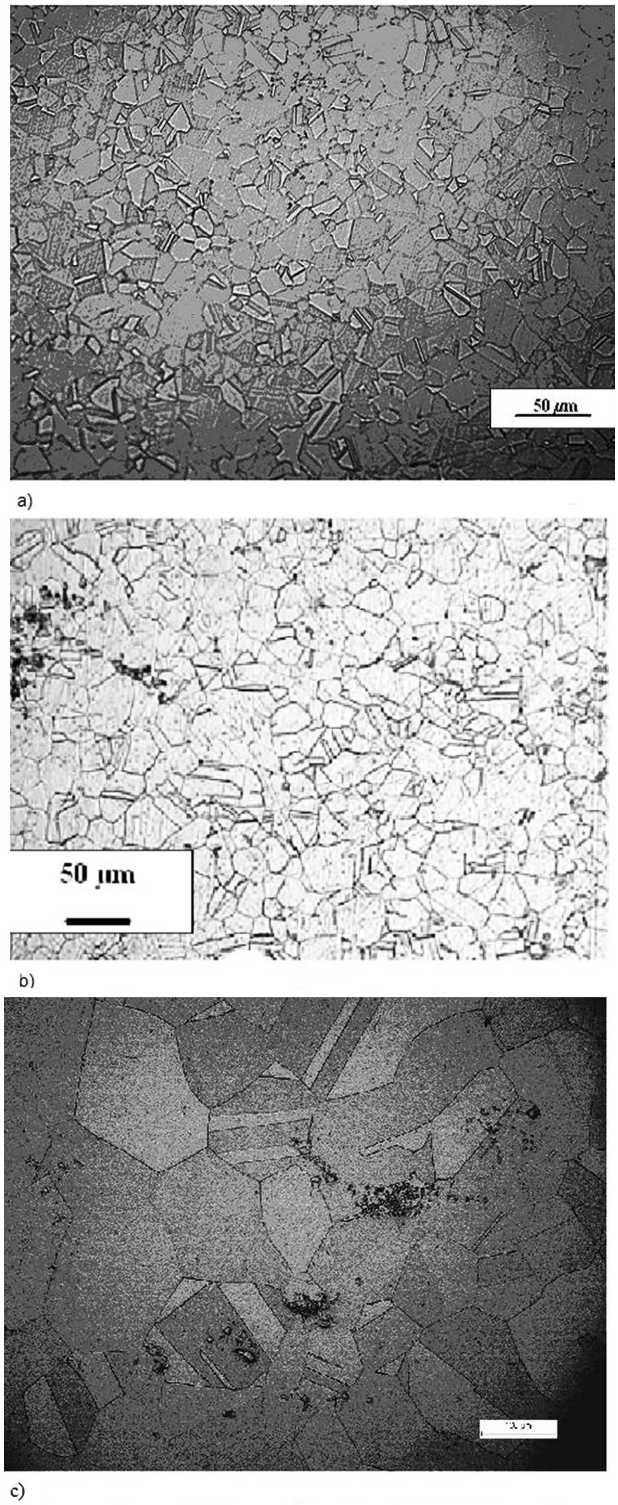

Fig. 2. a) Optical micrograph (microstructure) of the as-received superalloy; b) Optical micrograph for the superalloy annealed at 1323K/2h; c) Optical micrograph for the superalloy annealed at 1473K/2h

3.2. Data Analysis

The graphical plot in Fig. 3 enables us to analyze grain size data of the annealed samples as well as to discuss the various trends in the kinetics of grain growth for the investigated superalloy. The grain size for the as-received superalloy was measured (from optical micrograph) to be around 14 μm; which is close to the value measured from SEM micrograph (15.5 μm). Since a larger number of grains were considered in the measurement of grain size (by using line intercept method) in optical micrograph, the grain size = 14 μm, being more accurate, is chosen for the as-received superalloy. A comparison of the grain size of the as-received sample (14μm) with those for the annealed samples (50μm and 150μm) clearly indicates a definite grain growth in the annealed samples of the superalloy (see Fig. 3).

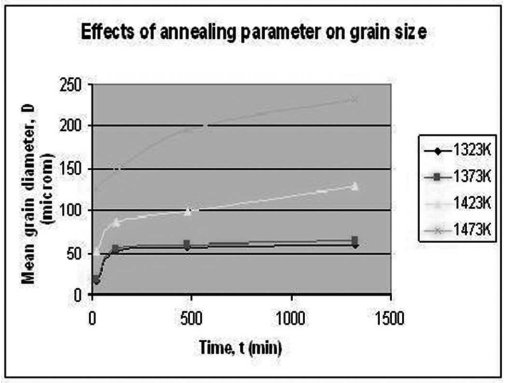

Fig. 3. Effects of temperature and time on the grain size of superalloy

The isothermal curves in the graphical plot (Fig. 3) indicate two interesting kinetic behaviors of grain growth. Firstly, the grains first grow rapidly and then more slowly with an increase in grain size at a particular temperature. This trend of grain growth establishes that the rate of grain growth decreases with an increase in grain size. Secondly, the lower temperature (1323K and 1373K) curves become almost horizontal for long annealing durations; whereas the higher temperature (1423K and 1473K) curves have relatively higher slopes for long annealing durations.

Now we quantitatively establish the kinetics of grain growth in the investigated superalloy. By application of Equation (3), the grain growth exponent, n was computed with the aid of graphical plots for temperatures in the range of 1323-1473K (see Fig. 4). In Fig. 4, the isothermal curve (line) corresponds to a specific value of the grain-growth exponent; the slope of each curve (line) shows the value of the grain-growth exponent, n at a particular temperature. It is evident from the graphical analysis presented in Fig 4. that n values lie in the range of 0.067-0.206 for the investigated superalloy. Recently, Huda and co-workers (2011) have reported some quantitative aspects of grain growth in the 718 superalloy; however, the grain-growth kinetic behavior, at temperatures exceeding 1423K, is un-explained in the research report **[25]**. The present study, which is an extended work of the reported research, enables us to furnish an in-depth explanation of the grain-growth kinetics of the investigated superalloy. The log-log plots (Fig. 4) clearly indicate that each of the set of lower two curves (for 1323K & 1373K) and the set of higher two curves (for 1423K & 1473k) have slopes (n values) that are close to each other; however, there is a significant rise in the n value (from 0.07 to 0.18) for the 50K rise in temperature (from 1373 to 1423K).

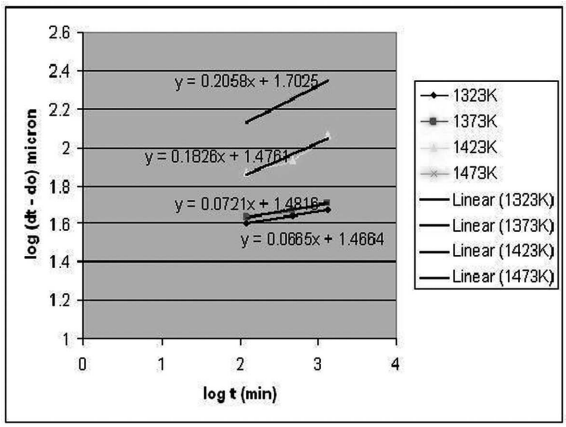

Fig. 4. Graphical plots of log ($D_t - D_0$) versus log t for the superalloy

Now, the grain-growth kinetic data for the investigated alloy is discussed in comparison to the data for other metals and alloys. For pure metals, the ideal grain growth exponent, n is 0.5 [**26**]. The lower n values (n=0.067-0.206) of the investigated superalloy as compared to those for pure metals (n=0.5) indicate that the grain growth process in the superalloy is highly restricted due to the solute drag effect on grain-boundary migration [22]. Additionally, n<0.4 is expected for a highly alloyed metal [**26**] and [**27**]. However, at high temperatures (here 1423-1473K), the n values have increased rapidly. This kinetic behavior of grain growth is justified owing to higher grain-boundary mobilities at higher annealing temperatures [22].

The rates of grain growth, G, at various temperatures have been calculated by using Equation (4). The G values for the time durations in the range of 2-8 hours were calculated because the values of G for the shortest period of annealing (20 min–2 h) showed no significant change in the grain size. By using Equation (4), the kinetic data for G at various temperatures (in the range of 1323-1473 K) were established; which are presented in Table 3. The G data indicates that the rate of grain growth increases with increasing temperature. Although there is no rise in the rate of grain growth, G, during annealing at temperatures in the range of 1323-1373K, the G value rises rapidly at 1423K and even more rapidly at 1473K (see Table 3). This kinetic behavior might be due to the higher mobilities of grain boundaries at higher annealing temperatures as discussed in the preceding paragraph.

TABLE 3
Rate of grain growth, G, for a duration from 2 to 8 hours at various temperatures

Temperature (K)	Rate of Grain Growth, G (m/s)
1323	1.85×10^{-10}
1373	1.85×10^{-10}
1423	5.56×10^{-10}
1473	2.27×10^{-9}

The kinetic data in Table 3 and use of Equation (4) enable us to compute the activation energy for grain growth, Q_g, as follows.

Equation (4) can be expressed in logarithmic form as:

$$lnG = lnG_o - (Q_g/RT) \tag{6}$$

Figure 5 shows graphical plot of *ln G* versus reciprocal of annealing temperature (1/T). The value of the gradient (slope) of the line in Fig. 5 enables us to compute the value of Q_g, as follows.

$$Slope = -\frac{Q}{R} = -52930 \tag{7}$$

$$Q_g = 8.31 \times 52930 = 439.8\, kJ/mol \tag{8}$$

Equation (8) leads us to conclude that the value of the activation energy, Q_g, for the investigated *Haynes*® 718 Ni-base superalloy, is around 440 kJ/mol for temperatures in the range of 1373-1473K.

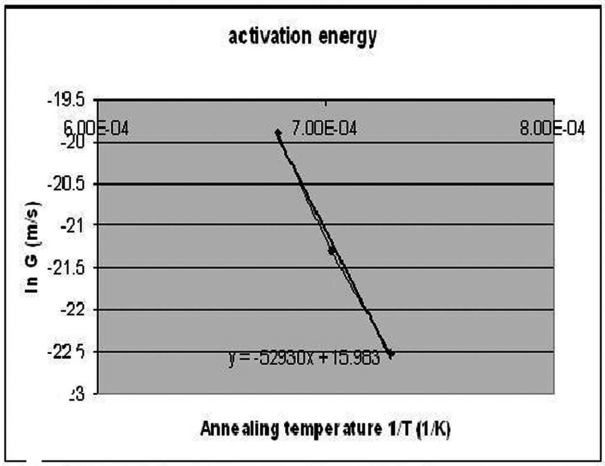

Fig. 5. Graphical plots of *ln G* versus reciprocal of annealing temperature

3.3. Comparative Analysis of Q_g

Now we compare the value of the activation energy for grain growth, Q_g computed for the investigated alloy with the values of Q_g for other alloys, reported in recent literature. Recently (2009), Cherukuri and co-workers have computed Q_g =320 kJ/mol for *beta-21S* titanium alloy [28]; which is lower than that of theQ_g value reported in the present paper. This material behavior can be justified in terms of the effect of solute on grain growth reported by Ralph and co-workers [22] as follows. The beta-21S titanium is a single-phase (solution annealed condition, resulting in a β structure) β-21S alloy containing only three solutes (alloying elements): Mo, Nb, and Si [29]. The solute drag effect on grain growth is relatively lower in the β-21S titanium alloy; which is why a lower energy per mol is required to activate grain boundaries. This explains the lower activation energy for grain growth (Q_g =320 kJ/mol) for *beta-21S* titanium alloy. On the other hand, the investigated 718 superalloy is a highly-alloyed material (see Table 1); which is why the solute drag effect on grain-boundary migration is more pronounced. This justifies a higher activation energy for grain growth (Q_g =440 kJ/mol) for the investigated superalloy.

Recently, researchers have reported Q_g =293.4 kJ/mol for a powder-metallurgy (P/M) superalloy [10]. The lower Q value as compared to the one reported in the present paper can also be justified in terms of a lesser solute drag effect on grain boundary migration because the P/M superalloy investigated by Tian and co-workers [10] is low-alloyed (whereas Haynes 718 superalloy is highly alloyed). Huda and Ralph (1990) have reported an activation energy for grain growth Q_g = 384 kJ/mol for a highly-alloyed APK-6 (a unique modification of IN-792) powder- metallurgy (P/M) superalloy [12]. The higher activation energy (Q_g =440 kJ/mol) for the investigated (rolled) superalloy as compared to those for P/M superalloys can be justified in view of research reported by Randle and co-workers (1986); who have identified a textural influence as a cause of grain-growth suppression [30]. Obviously, annealing twins can be clearly observed in the microstructure of sample A-2 (annealed at 1423K/2h) (see Fig. 2(b)); which indicates a textural influence to the grain growth process. This is why higher energy per mole is required to activate grain boundaries for grain growth; this explanation justifies the higher Q_g value for the investigated superalloy.

In fact, the activation energy for grain growth, Q_g, not only depends on solutes but also on second-phase particle-pinning effect as well as on recrystallization temperature (which in turn depends on melting temperature of the alloy). Nieh and Wadsworth (1989) have reported a high Q_g value (550 kJ/mol) for an engineering ceramic: Y_2O_3 stabilized ZrO_2 [31]; thereby indicating that Q values are higher for higher melting-temperature materials. Recently, Huda and Zaharinie (2009) have reported Q_g =157 kJ/mol for 2024-T3 aluminum alloy [21]. This Q value is about one-third of the Q value for the investigated superalloy. The lower Q value for the Al alloy can be justified in terms of the lower (about one-third) melting temperature of the Al alloy as compared to the superalloy.

4. Conclusions

It was established that for long-duration annealing at lower temperatures (1323 and 1373K), the grain growth was more restricted as compared to those at higher temperature (1423K and 1473K). This kinetic behavior has been justified in terms of higher grain-boundary mobilities at higher annealing temperatures. The grain-growth exponent, *n* was computed to be in the range of 0.067-0.206; the deviation from ideal (n=0.5) kinetic behavior was justified in terms of the solute drag effect on grain-boundary migration in the highly-alloyed 718 superalloy. The activation energy for grain growth, Q_g for the superalloy was computed to be 440 kJ/mol; the computed Q value was compared with those for titanium and aluminum alloys, ceramics, and other superalloys; and appropriate scientific explanations have been proposed.

Acknowledgements

The authors are also grateful to I.P.P.P unit, University of Malaya, Malaysia for *PJP* financial grant (Project No. FS124/2008B), awarded during 2008, for the research reported in the paper.

REFERENCES

[1] J. Tiley, G.B. Viswanathan, R. Srinivasan, R. Banerjee, D.M. Dimiduk, H.L. Fraser, Coarsening kinetics of γ' precipitates in the commercial nickel base Superalloy René 88 DT, Acta Mater. **57**(8), 2538-2549 (2009).

[2] K.Y. Cheng, C.Y. Jo, D.H. Kim, T. Jin, Z.Q. Hu, Influence of local chemical segregation on the γ' directional coarsening behavior in single crystal superalloy CMSX-4, Mater. Charact. **60**(3) 210-218 (2009).

[3] P.C. Xia, J.J. Yu, X.F. Sun, H.R. Guan, Z.Q. Hu, Influence of thermal exposure on γ' precipitation and tensile properties of DZ951 alloy; Mater. Charact. **58**(7), 645-651 (2007).

[4] K. Song, and M. Aindow, Grain growth and particle pinning in a model Ni-based superalloy, Mat. Sci. & Eng. A **479**, 365-372 (2008).

[5] H.J. Penkalla, J. Wosik, A. Czyrska-Filemonowicz, Quantitative microstructural characterisation of Ni-base superalloys, Mater. Chem & Phys. **81**(2-3), 417-423 (2003).

[6] H. Monajati, M. Jahazi, R. Bahrami, S. Yue, The influence of heat treatment conditions on γ' characteristics in Udimet® 720, Mat. Sci. Eng. A **373**, 286-293 (2004).

[7] R.S. Moshtaghin, and S. Asgari, Growth kinetics of γ' precipitates in superalloy IN-738LC during long term aging, Materials & Design **24**(5), 325-330 (2003).

[8] C. Slama, and M. Abdellaoui, Structural characterization of the aged Inconel 718, J. Alloys and Compounds **306**(1-2), 277-284 (2000).

[9] V. Randle, B. Ralph, Interactions of grain boundaries with coherent precipitates during grain growth, Acta Metallurg. **34**(5), 891-898 (1986).

[10] G. Tian, C. Jia, J. Liu, and B. Hu, Experimental and simulation on the grain growth of P/M nickel-base superalloy during the heat treatment process, Materials & Design **30**(3), 433-439 (2009).

[11] Z. Huda, Influence of Particle Mechanisms on the Kinetics of Grain Growth in a P/M Superalloy, Mater. Scie. Forum **467-470**, 985-990 (2004).

[12] Z. Huda, and B. Ralph, Kinetics of Grain Growth in P/M IN-792 Superalloy', Mater. Charact. **25**(2), 211-220 (1990).

[13] B. Radhakrishnan, and R.G. Thompson, Kinetics of Grain Growth in the Weld HAZ of Alloy 718, Metallurg. Trans A **24A**, 2773-2785 (1993).

[14] Z. Huda, Metallurgical Failure Analysis for a Blade Failed in a Gas-Turbine Engine of a Power Plant, Materials and Design **30**, 3121-3125 (2009).

[15] Z. Huda, Development of Heat Treatment Process for a P/M Superalloy for Turbine Blades, Materials and Design **28**(5), 1664-1667 (2007).

[16] Z. Huda, Development of Design Principles for a Creep-Limited Alloy for Turbine Blades', J. Mater. Eng. & Perf. **4**(1), 48-53 (1995).

[17] C.T. Sims, N.S. Stoloff, and W.C. Hagel, Superalloys II, John Wiley & Sons (1987).

[18] L. Xiaoa, D.L. Chenb, and M.C. Chaturvedia, Effect of boron and carbon on thermomechanical fatigue of IN 718 superalloy: Part I. Deformation behavior, Mater. Sci. Eng. A **437**, 157-171 (2006).

[19] R.E. Hummel, Understanding Materials Science: History, Properties, Applications. Springer, USA (2004).

[20] C. Suryanarayana, Mechanical Alloying and Milling, CRC Press, USA (2004).

[21] Z. Huda and T. Zaharinie, Kinetics of Grain Growth in2024-T3: an Aerospace Aluminum Alloy, J. Alloys and Compounds **478**, 128-132 (2009).

[22] B. Ralph, K.B. Shim, Z. Huda, J. Furley, M. Edirisinghe, Effect of Particles and Solutes on Grain-Boundary Migration and Grain Growth, Materials Science Forum **94-96**, 129-140 (1992).

[23] Z. Huda, Grain Growth in a Powder-Formed Nickel-base Superalloy, Ph.D Thesis (1991) Brunel University of West London, U.K.

[24] P. Cotterill, and P.R. Mould, Recrystallization and Grain Growth in Metals, University of Surrey Press, UK (1976).

[25] Z. Huda, T. Zaharinie, and S.H. Islam, Effects of Annealing Parameters on Grain Growth Behavior of Haynes 718 Superalloy, Int. Journal of Physical Sci. **6**(30), 7073-7077 (2011).

[26] C.T. Simpson, K.T. Aust, and W.C. Winegard, The four stages of grain growth, Met. and Mater. Trans. *B* **2(4)**, 987-993 (1971).

[27] T. Takasugi, and O. Izumi, Recrystallization and grain growth of Co_3Ti, Acta Metallurg. **33**, 49-58 (1985).

[28] B. Cherukuri, R. Srinivasan, S. Tamirisakandala, D.B. Miracle, The influence of trace boron addition on grain growth kinetics of the beta phase in the beta titanium alloy Ti-15Mo-2.6Nb-3Al-0.2Si, Scripta Materialia **60**(7), 496-499 (2009).

[29] D. Eliezer, E. Tal-Gutelmacher, C.E. Cross, Th. Boellinghaus, Hydrogen trapping in β-21S titanium alloy, Mater. Sci. Eng: A **421**(1-2), 200-207 (2006).

[30] V. Randle, B. Ralph, and N. Hansen, Grain growth in crystalline materials. Annealing Processes – Recovery, Recrystallization and Grain Growth, in Proc. 7^{th} Risφ Int. Symp. 1-8 (1986).

[31] T.G. Nieh, and J. Wadsworth, Biaxial gas-pressure forming of a superplastic Al_2O_3/YTZP, J. Amer Ceramic Soc, Vol. 72, Page 1469 (1989).

Received: 20 February 2013.